STUDY ON MEMS GLASSBLOWN CELLS FOR NMR SENSORS

Radwan M. Noor, Nikita Kulachenkov, Mohammad H. Asadian, and Andrei M. Shkel
MicroSystems Laboratory, University of California, Irvine, CA 92697, USA
Email: {rmmohamm, nkulache, asadianm, ashkel}@uci.edu

***Abstract*—This paper presents a study on factors that affect the relaxation rates of noble gas atoms in miniaturized atomic vapor cells of Nuclear Magnetic Resonance (NMR) sensors. The cells are implemented using the micro-glassblowing process, [1]. Our study is focused on the cell construction material and the inner wall coating of the cells. We showed that the wafer-level coating process with Al2O3 increased the 131Xe relaxation time (T2) by 4x and by switching from Borosilicate glass (Pyrex) to Aluminosilicate glass (ASG) T2 improved by 3x, for the same species. The improvement in T2 is projected to reduce the ARW of an NMR gyro by 4x and 3x with Al2O3 coated cells and ASG cells, respectively.**

***Index Terms*—Atomic sensors, microfabrication, nuclear magnetic resonance (NMR), gyroscopes, glassblowing, atomic cells, relaxation time.**

I. Introduction

Miniaturization of atomic vapor cells is a critical technology for chip-scale hot and cold atomic-microsystems. These microsystems include, but are not limited to, chip-scale magnetometers, clocks, and gyroscopes. We previously introduced the fabrication and filling processes of micro-glassblown spherical cells with alkali metal (Rb), noble (Xe) and buffer gases (Ne, N_2) on a wafer level, [2], [3]. In this paper, we present a study of cell geometry effects on relaxation rates of Xe atoms in micro-glassblown cells. Specifically, we focus on the inner wall coating and glass material.

The relaxation time of the noble gas atoms is directly related to the performance of NMR sensors. For gyroscopes, for example, the angle random walk (ARW) is predicted to depend on T_2 time as follows, [4],

$$ARW = \frac{3600}{T_2 \times SNR\sqrt{\delta f}}[^\circ/\sqrt{hr}],$$

where T_2 is the transverse relaxation time of the Xe atoms, SNR is the signal-to-noise ratio of the electron paramagnetic resonance (EPR) magnetometer, and δf is the bandwidth of the phase noise in Hz. Several factors can affect the relaxation rate of the noble gas atoms in atomic vapor cells, including collisions with alkali metal atoms, collisions with cell walls, magnetic field in-homogeneity inside the cell, and self-collisions of Xe atoms. In mm-sized cells, the wall collisions and spin exchange relaxation are dominant, [5], and therefore a special care needs to be taken during the cell construction.

This work was supported in part by the Defense Advanced Research Projects Agency (DARPA) under Contract W31PQ-13-1-0008, by the National Science Foundation under Award 1355629 and by Agency for Defense Development (ADD) under Award ADD-208376.

The work of R. M. Noor was supported by King Abdulaziz City for Science and Technology (KACST)

The work of N. Kulachenkov was supported by State Research Center of the Russian Federation Concern CSRI Electropribor, JSR, St. Petersburg, Russia

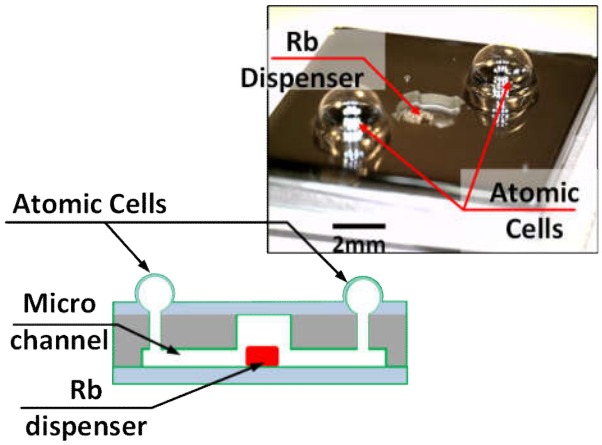

Fig. 1. Sketch of an atomic cell cross-section, showing two cells, a Rb dispenser, and micro channels. Insert: Example of a fabricated prototype showing the Rb dispenser and the vapor cells.

II. Fabrication

A. Fabrication Process

The fabrication process starts by etching 900 μm cavities in a 1 mm thick Si wafer, Fig. 2-(a). Next, the first anodic bonding seals the etched cavities under atmospheric pressure, Fig. 2-(b). After placing the wafer stack in a high temperature furnace at 850 °C for Borosilicate glass (Pyrex) and 1000 °C for Aluminosilicate glass (ASG) for 5-7 minutes, spherically shaped glass shells are formed, [6], Fig. 2-(c). The formation was due to two effects: the trapped air inside the cavities builds up the pressure due to the temperature increase, and the glass transitions from a solid state to a viscous state.

The next step in the process was to open the backside of Si wafer and to define 100μm deep micro-channels using DRIE etching, Fig. 2-(d). Next, the cell coating was applied via atomic layer deposition (ALD) of 10 nm aluminum oxide (Al_2O_3) to the opened cells and the capping wafer, Fig. 2-(e).

The second anodic bonding took place after the alkali dispenser pills have been placed in the central cell, with the ALD Al_2O_3 as an intermediate layer between the backside

978-1-5386-7828-2/19/$31.00 ©2019 IEEE

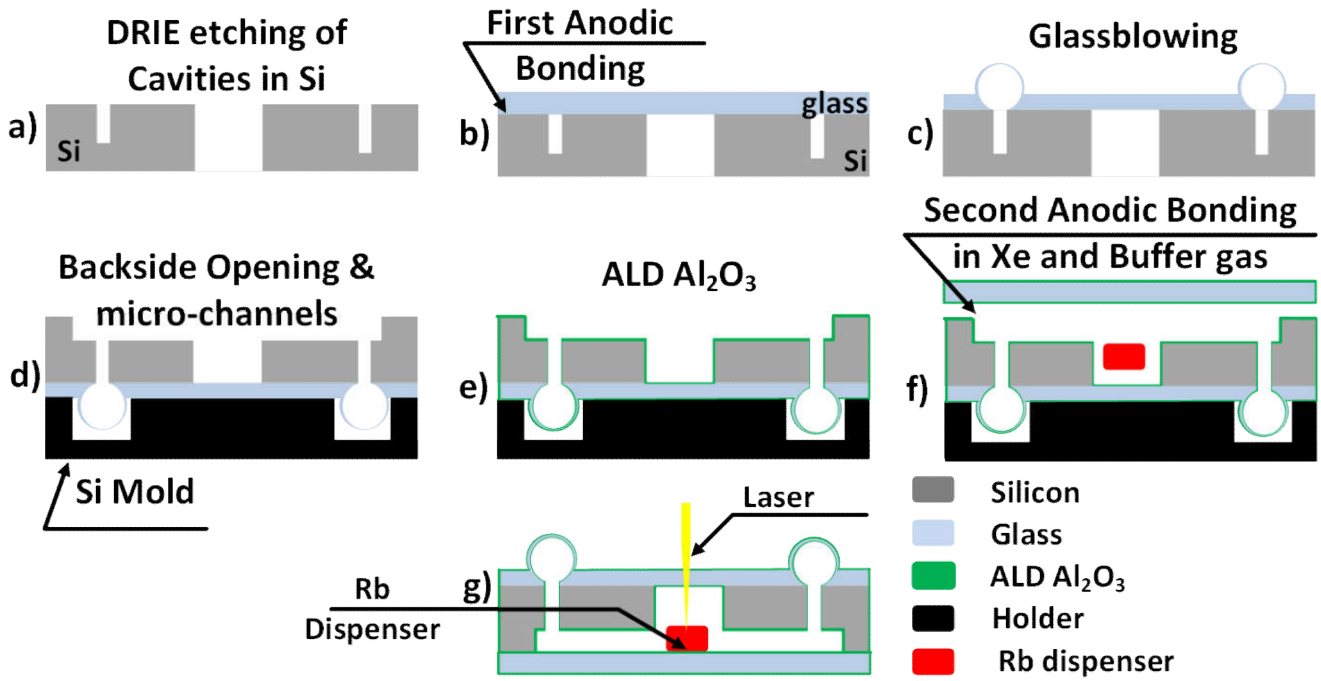

Fig. 2. Description of the process flow: (a) DRIE etching of 900μm and through wafer cavities in 1mm Si wafer, (b) first anodic bonding of glass to the etched Si wafer, (c) glassblowing of cells, (d) cell back-side opening and channel definition using DRIE etching, (e) Atomic Layer Deposition (ALD) of 10nm Al_2O_3, (f) loading the Rb dispenser and performing the second anodic bonding in a noble gas and buffer gas filled chamber, (c) Dispensing Alkali metal through micro channels by Laser heating of Rb source

of the Si wafer and the capping glass wafer, Fig. 2-(f) . The wafer alignment for bonding was performed inside a chamber with a noble gas and a buffer gas at pressure of 250-350 Torr, Fig. 2-(f). After the bonding process was complete, each dispenser was activated by focusing a 3.5-4W laser for 15 seconds, which released the alkali vapor to satellite cells, Fig. 2-(g).

B. Coating

Alkali metals, like Rb, react with glass cells at elevated temperatures, which leads to a consumption of the metal. One method to reduce this interaction is by passivating the glass walls of the cells. In, [7], it was shown that a 20nm layer of Al_2O_3 can reduce the interaction between alkali metals and cell glass walls by 100x. In, [7], it was also found that anodic bonding worked with ALD Al_2O_3 as an intermediate layer. This paper intended to examine these claims.

ALD is a thin film conformal coating technique, the reaction of two chemicals in a gas phase with a surface creates one atomic layer, for example, Trimethylaluminum (TMA) and H_2O create Al_2O_3. The process is self-limiting to a single atomic layer per cycle. The coating is achieved by repeating deposition cycles until the desired thickness is reached. In our study, we used a commercial instrument by Cambridge nanotech to deposit 10 nm of Al_2O_3, on both the sample and the capping wafer. The deposition parameters are summarized in Table I .

TABLE I
SUMMARY OF ALD Al_2O_3 DEPOSITION PARAMETERS

	pulse time(s)	purge time(s)	N_{cycles}	N_2 rate [sccm]	Temp (°C)
TMA	0.015	10	100	20	200
H_2O	0.05	10	100	20	200

III. Experimental Results

All the fabricated cells used in this study were filled with similar amounts of noble and buffer gasses. The pressure values at room temperature were: for natural Xe at 65 torr, for Ne at 45 torr, and for N_2 at 300 torr. A data fitting of the Rb absorption curve (obtained by sweeping the wavelength of the VCSEL beam passing through the cell) was used to confirm the amount of noble and buffer gasses inside the cell. Measurements showed a significant reduction of the N_2 gas pressure, 85%-90%, due to absorption by the getter material in the Rb pill. The experimentally measured relaxation time (T_2) of ^{129}Xe and ^{131}Xe isotopes were used to compare cells. The cells were heated optically using a 2.5W laser source at 1550nm, focusing only on the Si part of the cell substrate. We used the free induction decay (FID) method to estimate the relaxation rate using a dual beam scheme, one for pumping and another for detection, Fig. 3.

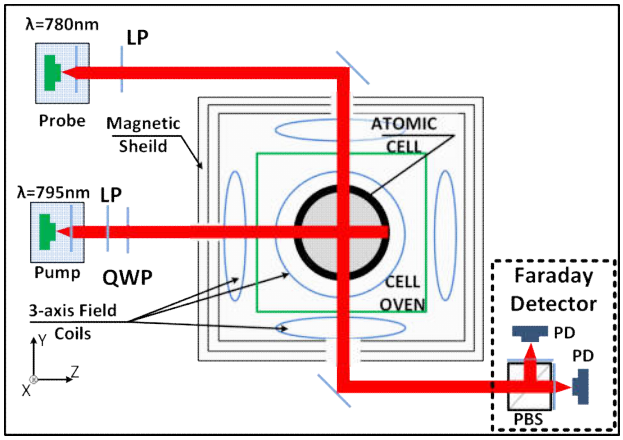

Fig. 3. Dual beam optical setup for characterization of cells. (LP: linear polarizer, QWP: quarter wave plate, PBS: polarizing beam splitter, PD: photo detector, Faraday Detector: a balanced polarimeter used to detect Faraday Rotation)

A. Gas Content Measurement

Buffer and noble gasses contribute to the Rb transition line by broadening the light absorption spectrum and shifting the frequency of absorption by specific values for each gas, reported in [8] and [9]. The absorption data were fitted to the Lorentzian function defined as

$$F(x) = ax + b - 1/\pi \sum_{i=1}^{4} \frac{c_i \Gamma_i}{(x - x_i)^2 + \Gamma_i^2}$$

where a and b are parameters of a line. For each of the two ground transitions of ^{85}Rb and ^{87}Rb, x_i is the center frequency of that transition in MHz, Γ_i is the broadening of that peak in MHz, c_i is a constant representing the amplitude of the peak (depth).

The Rb dispenser that was used in our process consisted of a pure alkali metal and a getter material. Once the dispenser was activated, the alkali metal was released and the getter material started to absorb active gasses, such as O_2, H_2O, N_2. To estimate the amount of remaining N_2 gas, we started by splitting a laser beam in half and passing the two beams, one to a reference cell with only natural Rb and the other to our fabricated cell with Rb and other gasses. By sweeping the laser wavelength, we obtained two Rb light absorption spectrum curves, one for the reference cell, where the two ground transitions of each isotope ^{85}Rb and ^{87}Rb could be distinguished, the other is for the fabricated cell, where these transitions had been broadened and shifted due to the buffer gasses, [8], [9]. Starting with the Rb light absorption spectrum of the reference cell and substituting for the broadening and frequency shift rates of Xe and Ne in an iterative curve fitting, we were able to find the N_2 pressure that resulted in a matching Rb light absorption spectrum curve of the fabricated sample on hand.

B. Experimental Setup

The atomic cell was placed in a miniaturized oven made from a thermal insulating material, all housed by a nested 4-layer μ-metal shield with integrated 3-axis magnetic field coils. The pump beam of 2.5mW with acircularly polarized light locked on Rb D1 line (795nm) along the z-axis. A DC field of 3.5μT and an RF field of 17.8kHz with an RMS amplitude of 3.5μT were applied along the z-axis. The probe beam was a linearly polarized beam of 1mW set off- resonance from D2 line (780nm) and was applied along the y-axis. The produced RF signal was used as a reference for the lock-in amplifier that demodulated the output of the Faraday detector at the probe side (Faraday Detector is a balanced polarimeter used to detect Faraday Rotation). A $\pi/2$ pulse at the frequency of the Xe isotope of interest was applied along the y-axis to obtain the FID signal, which was fitted to an exponentially damped sine wave to extract the relaxation time T_2. Fig. 4 shows an example of the FID signal for ^{131}Xe.

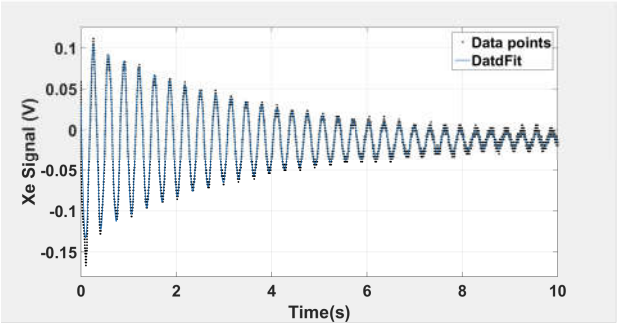

Fig. 4. Example of FID Signal of ^{131}Xe isotope.

TABLE II
SUMMARY OF CELLS USED IN THIS STUDY AND THE CORRESPONDING RELAXATION TIMES OF EACH ISOTOPE

Cell	**1**	**2**	**3**
Glass	Pyrex	Pyrex	ASG
Coating	n/a	10nm Al_2O_3	n/a
^{129}Xe T_2 **(s)**	1.4	0.79	1.2
^{131}Xe T_2 **(s)**	0.74	3.55	2.35

C. Results

In this study, we measured T_2 for both isotopes at different temperatures for all cells, Fig. 5 and Fig. 6. Table II summarizes the studied parameters and the average relaxation time of ^{129}Xe and ^{131}Xe isotopes in the range from 115°C to 140°C. We observed that Atomic Layer Deposition (ALD) of 10 nm Al_2O_3 on the cell walls increased the transverse relaxation time of the ^{131}Xe isotope by a factor of 4.7x, when compared to cells without coating. When using an Aluminosilicate glass (ASG) instead of Borosilicate glass (Pyrex), we observed a similar effect on the relaxation time of ^{131}Xe isotope, demonstrating an increase of T_2 by a factor of 3.2x. We did not observe the quadruple frequency splitting with the ^{131}Xe in any of the micro-glassblown cells. We believe this is due to symmetry of the cells and the fact that the active area of the cell is made from the same material, which agrees with conclusions in [10]. On the other hand, ALD coating of

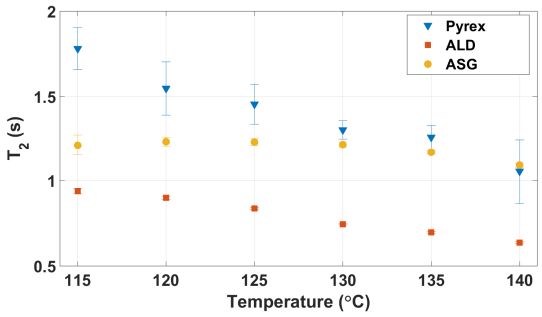

Fig. 5. Comparison of Transverse relaxation time T_2 vs temperature of 3 different samples (Pyrex: triangles, Pyrex with Al_2O_3 coating: squares, and aluminosilicate glass ASG: circles) for ^{129}Xe isotope, showing the effect of ALD coating on T_2. Error bars represent the standard deviation of the measured T_2 values over ten consecutive measurements.

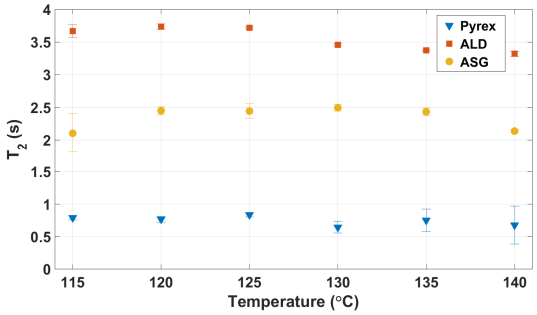

Fig. 6. Comparison of Transverse relaxation time (T_2) vs temperature of 3 different samples (Pyrex: triangles, Pyrex with Al_2O_3 coating: squares, and aluminosilicate glass ASG: circles) for ^{131}Xe isotope, showing the improvement of using ASG glass and ALD coating. Error bars represent the standard deviation of the measured T_2 values over ten consecutive measurements.

Al_2O_3 was found to reduce the relaxation time of the ^{129}Xe isotope by a factor of 2x, while the ASG glass did not show a significant difference in T_2 of ^{129}Xe, as shown in table II.

Assuming a SNR of 2500, the projected ARW of NMR gyro for ^{131}Xe species decreased from 2 $°/\sqrt{hr}$ to 0.4 $°/\sqrt{hr}$ for Al_2O_3 coated cells and to 0.6 $°/\sqrt{hr}$ for cells made with ASG glass, Fig. 7.

IV. Conclusion

In conclusion, we investigated the effect of the atomic vapor cell wall construction parameters, fabricated using micro-glassblowing technique [1], utilizing the transverse relaxation times T_2 of noble gas of Xe isotopes as a control parameter. Specifically, we studied the inner wall coating as well as the cell glass material. We found that 10nm ALD Al_2O_3 increased T_2 of ^{131}Xe by 4.7x and decreased the T_2 of ^{129}Xe by 2x. We also found that using ASG glass instead of Pyrex increased T_2 of ^{131}Xe by 3.2x and did not have a significant impact on the T_2 of ^{129}Xe. In light of the experimental results and the analytical model of the NMRG ARW, [4], for example, and assuming the same SNR value, the Al_2O_3 coating is projected to reduce the NMRG ARW by more than 4 fold.

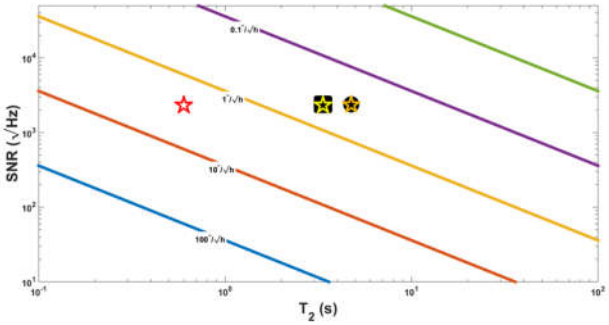

Fig. 7. ARW of NMR gyro based on ^{131}Xe and assuming 2500 SNR, shows the projected ARW reduction as a result of T2 improvement. (Initial ^{131}Xe T_2 (red star), T_2 of Al_2O_3 coated cell (circle) and ASG glass cell (square))

Acknowledgments

Devices were designed, developed, and tested in MicroSystems Laboratory, UC Irvine. The authors would like to thank UCI INRF staff for their help with the fabrication, Dr. Larsen, and Mr. Bulatowicz for suggestions on improvement of the characterization setup.

References

[1] E. J. Eklund, A. M. Shkel, S. Knappe, E. Donley, and J. Kitching, "Spherical rubidium vapor cells fabricated by micro glass blowing," in *IEEE Conference on Micro Electro Mechanical Systems (MEMS'07).*, (Kobe, Japan), January 21-25, 2007.

[2] R. M. Noor, V. Gundeti, and A. M. Shkel, "A status on components development for folded micro NMR gyro," in *2017 IEEE International Symposium on Inertial Sensors and Systems (INERTIAL'17)*, (Kauai, HI USA), March 28-31, 2017.

[3] R. M. Noor and A. M. Shkel, "MEMS components for NMR atomic sensors," *IEEE Journal of Microelectromechanical Systems*, vol. 27, no. 6, pp. 1148–1159, 2018.

[4] I. Greenwood and J. Simpson, "Fundamental noise limitations in magnetic resonance gyroscopes," in *NAECON'77; Proceedings of the National Aerospace and Electronics Conference*, (Dayton, OH USA), May 17-19, 1977.

[5] J. Kitching, "Chip-scale atomic devices," *Applied Physics Reviews*, vol. 5, no. 3, p. 031302, 2018.

[6] E. J. Eklund and A. M. Shkel, "Glass blowing on a wafer level," *IEEE Journal of Microelectromechanical Systems*, vol. 16, no. 2, pp. 232–239, 2007.

[7] S. Woetzel, F. Talkenberg, T. Scholtes, R. IJsselsteijn, V. Schultze, and H.-G. Meyer, "Lifetime improvement of micro-fabricated alkali vapor cells by atomic layer deposited wall coatings," *Surface and Coatings Technology*, vol. 221, pp. 158–162, 2013.

[8] M. D. Rotondaro and G. P. Perram, "Collisional broadening and shift of the rubidium d1 and d2 lines (52s12, 52p12, 52p32) by rare gases, h2, d2, n2, ch4 and cf4," *Journal of Quantitative Spectroscopy and Radiative Transfer*, vol. 57, no. 4, pp. 497–507, 1997.

[9] G. A. Pitz, A. J. Sandoval, T. B. Tafoya, W. L. Klennert, and D. A. Hostutler, "Pressure broadening and shift of the rubidium d1 transition and potassium d2 transitions by various gases with comparison to other alkali rates," *Journal of Quantitative Spectroscopy and Radiative Transfer*, vol. 140, pp. 18–29, 2014.

[10] E. Donley, J. Long, T. Liebisch, E. Hodby, T. Fisher, and J. Kitching, "Nuclear quadrupole resonances in compact vapor cells: the crossover between the NMR and the nuclear quadrupole resonance interaction regimes," *Physical Review A*, vol. 79, no. 1, p. 013420, 2009.